Sato, Yuki; Noreikis, Marius; Xiao, Yu

Low-cost mapping of RFID tags using reader-equipped smartphones

Published in:
Proceedings of the 15th IEEE International Conference on Mobile Ad-hoc and Sensor Systems

DOI:
10.1109/MASS.2018.00052

Published: 01/01/2018

Document Version
Peer-reviewed accepted author manuscript, also known as Final accepted manuscript or Post-print

Please cite the original version:
Sato, Y., Noreikis, M., & Xiao, Y. (2018). Low-cost mapping of RFID tags using reader-equipped smartphones. In *Proceedings of the 15th IEEE International Conference on Mobile Ad-hoc and Sensor Systems* (pp. 299-307). (IEEE International Conference on Mobile Ad-hoc and Sensor Systems). IEEE. https://doi.org/10.1109/MASS.2018.00052

Low-cost mapping of RFID tags using reader-equipped smartphones

Yuki Sato, Marius Noreikis, Yu Xiao
Department of Communications and Networking, Aalto University
Konemiehentie 2, Espoo, Finland
Email:{sato.yuki, marius.noreikis, yu.xiao}@aalto.fi

***Abstract*—This paper proposes a low-cost solution for mapping and locating UHF-band RFID tags in a 3D space using reader-equipped smartphones. Our solution includes a mobile augmented reality application for data collection and information visualization, and a cloud-based application server for calculating locations of the reader-equipped smartphones and the read RFID tags. Our solution applies computer vision and motion sensing techniques to track 3D locations of the RFID reader based on the visual and inertial sensor data collected from the companion smartphones. Meanwhile, it obtains the exact locations of RFID tags by calculating their relative positions from the readers based on the Angle of Arrival (AoA) concept. Our solution can be implemented with any low-cost fixed transmit power RFID readers, since it only requires the readers to report identifiers of read RFID tags. Furthermore, our solution does not require machine-controlled uniform movement of RFID readers, as it can handle the bias in the readings collected from randomly scattered positions. We have evaluated our solution with experiments in real environments using a commercially-off-the-shelf RFID reader and an Android phone. Results show that the average error in the positions of RFID tags is around 25cm for each of orthogonal axes on the floor plane, with the orders of RFID tags correctly detected in most cases.**

***Index Terms*—RFID, localization, smartphone, augmented reality**

I. Introduction

Ultra high frequency (UHF)-band radio frequency identification (RFID) tags have been widely used for object localization in applications for inventory management. The localization of RFID tags can be divided into two categories. One is absolute object localization that tells the exact positions of RFID tags, while the other is relative object localization that detects the order of RFID tags in 2D dimensions based on their positions relative to the RFID readers [1]. Currently, the absolute localization mechanisms that can achieve small error margins require either dedicated hardware (e.g. array antennas or customized RFID readers with a software-defined radio) [2], [3] or multiple pre-deployed antennas as reference points [4], which makes them difficult and expensive to deploy.

In this work, we propose a low-cost object localization solution that maps RFID tags in a 3D space using smartphones equipped with UHF-band RFID readers. With our solution, people carrying a reader-equipped smartphone can walk through an area, for example a warehouse, to generate and update a map of RFID tags. Meanwhile, others can easily search for RFID tags based on the generated map. To achieve a low-cost implementation, our solution only requires RFID readers to be able to collect identifiers of RFID tags, which is the minimum functionality provided by any RFID reader.

Our solution includes a mobile augmented reality (AR) application for data collection and information visualization, and a cloud-based application server for calculating locations of the RFID readers and tags. Firstly, our solution utilizes videos captured by smartphone cameras to create a 3D model of an indoor space using Structure from Motion (SfM) techniques [5]. With the SfM-based 3D model, it can locate a reader-equipped smartphone with photos taken by the smartphone based on image feature matching. After the initial position is identified, it can also track the following locations of the phone using both vision and inertial sensor data. Secondly, the reader collects identifiers of RFID tags in its reading range, and sends it to the application server which calculates the positions of RFID tags relative to the reader based on the Angle of Arrival (AoA) concept. The algorithm assumes facing directions of the smartphone, i.e. that of reader's antenna, at the time of reading as the AoA of the RFID tags. The relative positions are converted into absolute positions in the 3D space, according to the location of the reader, i.e. that of the smartphone, at the time when the RFID tags are read. Finally, the mobile application supports RFID tag search, and can display the RFID identifiers on top of the tagged objects in an AR mode.

When reader's positions are not uniformly scattered around the RFID tags, the RFID localization algorithm produces biased estimation of their positions. To counter this problem, we developed a bias removal method using reference RFID tags. With this method, our solution requires neither installation of fixed-position RFID readers nor machine-controlled movement of them. According to our experiments in a library using commercially-off-the-shelf equipments, our solution can locate with a high accuracy the shelf segments where RFID-tagged objects are stored.

The contribution of this paper focuses on the development and evaluation of an absolute RFID localization mechanism that requires only a minimum functionality from RFID readers. With emerging adoption of UHF-band RFID tags, it is expected that consumer devices, such as smartphones, will be equipped with UHF-band RFID readers in the future, just like embedding near field communication (NFC) transceivers in smartphones today. Providing a low-cost solution for mapping and locating RFID tags becomes important in order to make benefits of RFID commonly available.

The rest of this paper is organized as the following. Section II introduces background and related work, and Section III describes the proposed system and details of algorithms composing it. Section IV presents the results of performance evaluation through 2 experiments: the first one evaluates the characteristics of the RFID localization algorithm, and the second one evaluates performance of the whole proposal in a real world environment. Section V concludes the paper.

II. Background and Related work

This section gives an overview of image-based indoor localization, and summarizes the related works in the field of RFID tag localization and mapping.

A. Image-based indoor localization

Indoor localization is a well studied, yet highly challenging and sparsely adopted technology in comparison with satellite based outdoor localization. Researchers have proposed indoor localization methods ranging from infrastructure based ones, such as ultra wide band [11], Wi-Fi [12] and Bluetooth [13] beacons, to infrastructure-less methods based on geomagnetic field measurements [14] or computer vision [5]. In this work we choose to utilize computer vision techniques to implement image-based localization.

There are several image-based localization techniques. Huang et al. [15] used panorama images and visual features matching to calculate positions of a user. Gerstweiler et al. [16] and Ventura et al. [17] utilized Visual Simultaneous Localization and Mapping (VSLAM) to estimate user's indoor position. Dong et al. [18] utilized SfM techniques for reconstructing 3D models from 2D images and implementing image-based localization. While VSLAM systems can ensure high accuracy for tracking user's position, SfM based approaches enable localization with a single image in complex environments.

Multiple open source tools for SfM were proposed in recent years [19], [20], [21]. Computing an SfM model involves several steps: 1) visual features, e.g. SIFT [22], are extracted from all input images; 2) the features are matched between every pair of images; 3) the matched 2D positions are triangulated into 3D points with a multi view geometry algorithm. The final model not only contains the 3D points but also positions and facing directions (also known as 6 Degrees-of-Freedom (DoF) poses) of all cameras that took the input images. When a new image is added to an existing SfM model, one can easily obtain its camera position and facing direction, thus making SfM a convenient technique for image-based localization. In our work we apply SfM based indoor localization [5] for obtaining initial positions of a reader-equipped smartphone, and then utilize visual and inertial sensors for a continuous tracking. More details about our localization algorithm are given in Section III-A.

B. RFID tag localization

Localization of RFID tags has been one of the most attractive topics in RFID area. Recent development in AR technologies also enables novel applications of the RFID tags localization. E.g. Rashid et al. [6] proposed an AR application which provides information of products on a smartphone screen based on their positions obtained from RFID tag localization. This subsection discusses the existing works on RFID tag localization from two perspectives: the required infrastructure and the required parameters of RFID readers, and compares our solution with the existing works in Table I.

Localization infrastructure: From the perspective of RFID tags localization, Rashid's system [6] requires installation of RFID readers with multiple antennas on shelves in order to locate products on them. Several commercial products realize such RFID localization with fixed-position readers, e.g. Impinj xArray[2] and Mojix STAR[23]. They utilize fixed-position RFID readers with multiple antennas, and some of them use antennas with additional functions such as beam forming. Ryoo et al. [4] proposed a system to locate RFID-tagged shopping carts with phase-based ranging technique using multiple channel frequency. Using multiple readers and their antennas attached on a ceiling, it achieves a localization accuracy of $10cm$. However, such approaches require large-scale deployment of dedicated infrastructure, thus imposing a high deployment cost.

Researchers have also studied RFID tag localization which does not require such large-scale deployment of fixed-position RFID readers. Shangguan et al. [1] proposed a relative localization method with RFID readers moving along ordered RFID tags. Profiling variation of backscattered signal's phase from RFID tags according to the changes of relative position from reader's antenna, their method achieves 84% accuracy in ordering RFID tags placed in a real environment with $3 \sim 8cm$ gap. Another work [9] utilized holography method, which collects reference data from known-position RFID tags at first, then finds positions of unknown RFID tags based on the similarity between the reference data and the same type of data for an unknown RFID tag. Using amplitude and phase of the backscattered signal at multiple channel frequency and reader's position as the holography, this work can handle the cases where there are smaller gaps between RFID tags. Zhang et al. [10] introduced an interesting idea which attaches 3 arrays of multiple RFID tags in orthogonal directions on an object. It can identify not only positions but also directions of the object by collecting phases of signals from these RFID tags at different positions of the reader's antenna. However, it is difficult to apply these techniques, because they require uniform movement of the RFID reader, which is not feasible for handheld devices.

Additional parameters of RFID readers: While the minimum functionality of RFID readers is collecting identifiers of RFID tags in their reading range, some commercially-off-the-shelf RFID readers can also report characteristics of backscattered signal from RFID tags. Such information, typically radio signal strength indicator (RSSI) and phase of the signal, are utilized in some of the above-mentioned existing works. Miyazawa et al. [8] proposed an AoA detection method based on phase difference between backscattered signals received by multiple antennas. It can estimate AoA of RFID tags in reading

TABLE I
COMPARISON ON REQUIREMENTS OF RFID TAG LOCALIZATION TECHNIQUES

	RFID reader placement and device requirement	Additional parameters from RFID readers
Rashid et al. [6]	Fixed reader with multiple antennas embedded in shelves	None
Ryoo et al. [4]	Fixed reader with multiple antennas on a ceiling	Phase
Zhang et al. [7]	Fixed reader which TPO can be widely configured	None
Ma et al. [3]	Fixed UWB reader (implemented with software defined radio)	Time of flight
Miyazawa et al. [8]	Mobile reader with multiple antennas and concurrent phase measurement	Phase
Shangguan et al. [1]	Reader moving along ordered RFID tags	Phase
Shangguan et al. [9]	Reader moving within a predefined course (implemented with a robot)	Phase, RSSI
Zhang et al. [10]	Reader which antenna takes multiple positions (implemented with a positioner)	Phase
Our solution	Mobile reader with a single antenna and fixed TPO, equipped on a smartphone	None

range from anywhere without any reference data. It relies on concurrent phase measurement on at least 2 or more antennas separated by a certain distance. Ma et al. [3] proposed a ranging method for RFID tags based on Time of Flights, which is basically an ultra wide band technique. Their method uses a special reader, which is implemented with USRP software defined radio platform in their experiments, but can be applied to general UHF-band RFID tags without any modification. However, utilizing these additional parameters limits a choice of RFID readers that can implement the techniques.

On the other hand, other existing works do not rely on such additional information. For instance, Zhang et al. [7] proposed a method to locate RFID tags based on comparison of reading probability of reference RFID tags and unknown RFID tags at various transmitter power output levels (TPO). The method uses only a single reader's antenna, but position and direction of the antenna need to be fixed. The requirement of various TPO also makes it difficult to implement this method on power-constrained handheld devices.

As listed in Table I, our solution does not require any fixed arrangement or uniform movement of RFID readers. In addition, it identifies positions of RFID tags that are read with fixed TPO of RFID readers. These features are not considered in the above-mentioned existing works, but are important for realizing a low-cost RFID mapping solution with reader-equipped smartphones.

III. SYSTEM OVERVIEW AND ALGORITHMS

The proposed system, as illustrated in Figure 1, is composed of the following types of components:

- **RFID tags** attached to items. Each RFID tag has its own unique identifier.
- **Smartphones equipped with RFID readers**. The antenna of RFID reader is attached to the back of the smartphone, where the antenna boresight and the smartphone's camera face the same direction, as shown in Fig.1. The position and direction of the smartphone are treated as those of RFID reader's antenna and its boresight (hereafter referred to as "reader's position" and "reader's direction"), respectively.
- **Mobile application**. The mobile application captures photos and sends them to the application server for calculating the initial reader's position and direction. After that, it continuously tracks reader's position and direction based on inertial and visual sensor data, and sends the updated position and direction to the server. It also displays real world positions of read RFID tags in an AR view. A list of identifiers of localized RFID tags and their positions can be retrieved from the server.
- **Cloud-based application server**. The server runs two algorithms. One is an image-based localization algorithm that calculates a 6 DoF camera pose - reader's position and direction - from an input image and sends it back to the smartphone. The other is a RFID localization algorithm that computes positions of each RFID tag based on reading records collected from reader-equipped smartphones. Each reading record contains a read identifier, reader's position and direction at the reading.

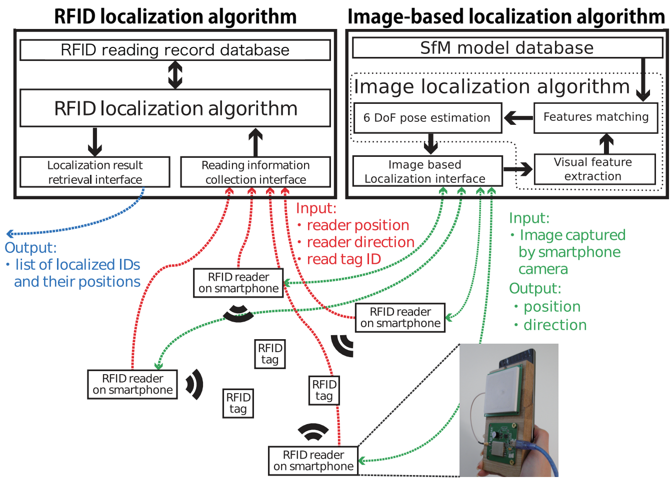

Fig. 1. System overview

A. Localization of RFID reader

We have developed an Android application for data collection and information visualization. When a user wants to start the mapping of RFID tags, she starts the mobile application on a reader-equipped smartphone and firstly locates the smartphone with an image. In order to enable image-based positioning, one has to shoot videos within premises, that would cover the area. The videos are then uploaded to a server, where we utilize techniques from our previous work [5] to build SfM models of the premises. The built models are

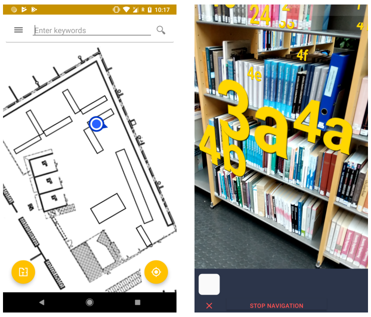

(a) User's position and facing direction shown on a library map

(b) Already recognized RFID tags in AR view

Fig. 2. Mobile application

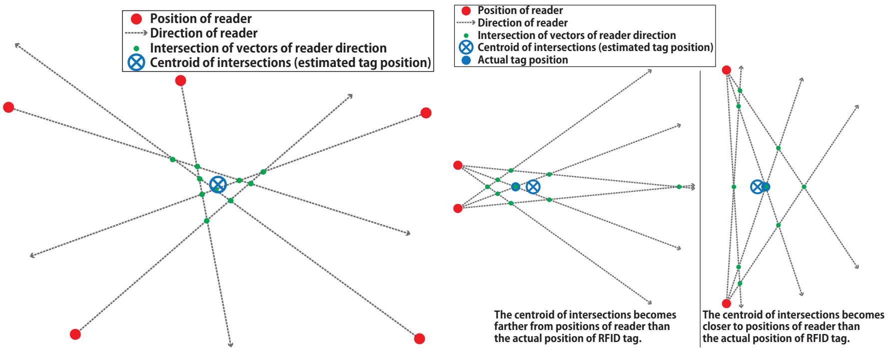

(a) Assuming a centroid of intersections between reading records as the position of RFID tag.

(b) Bias of reader's position towards a certain direction causes localization errors in the direction.

Fig. 3. Graphical description of the RFID localization algorithm

stored in a database, and are loaded when the image-based localization server is initiated. When a smartphone sends a query image to the image-based localization server, the server firstly extracts SIFT [22] features from the image, then matches them to a feature set of the already existing SfM model and finally utilizes matched features to estimate 6 DoF pose. We utilize a 6 points algorithms for final pose estimation [24]. The 6 DoF pose contains a 3D position as well as a 3D facing direction of a device and is an essential element to enable AR applications.

The application then shows the initial position and direction on a map (See Fig.2(a)). After that, the user starts a scanning mode, which switches application user interface to AR mode and sends continuous reader's position and direction updates to the server. Because the process of image-based localization is compute intensive and executed in a cloud [5], the position updates cannot be done in real time. Nevertheless, for AR based applications position and facing direction updates must be done in real time to ensure that augmented objects are correctly placed in real world and do not drift. Therefore, we utilize ARCore[1] technology to enable real time updates between subsequent image-based localization requests. ARCore runs on a smartphone and utilizes both inertial and visual sensors and is suitable for robustly tracking smartphone's position and facing direction for short periods of time. In this way we can ensure rapid and accurate position updates and a seamless AR experience. We evaluate the accuracy of image-based localization and ARCore tracking in Section IV-B.

AR mode is also useful for showing content in real world locations. Once a new RFID tag is identified by RFID localization algorithm, it is shown in the mobile app (Fig.2(b)). To implement the AR functionality in the application, we first show camera feed on the screen. We then utilize the results of image-based localization as well as the updates provided by the ARCore tracking algorithm to calculate positions of augmented objects to make sure they stay steady regarding the camera view feed and are properly aligned with real world objects - in our case, an augmented text is aligned with a shelf.

[1]https://developers.google.com/ar/discover/

B. Localization of RFID tags

Many existing localization methods for RFID tags employ either/both multiple dedicated antennas or/and measurements of physical characteristics of radio waves, such as RSSI and phase. Differently from them, our solution only requires RFID readers to collect identifiers of RFID tags using a single antenna. Thus, any reader can be used for implementing our solution.

Figure 3(a) illustrates how our RFID localization algorithm works. Its concept is based on AoA, i.e. estimating positions of RFID tags from directions where their responses come from. The proposal assumes that RFID tags are along readers' directions at the time when they are read, then tries to find intersections of those vectors for each identifier of an RFID tag. Two vectors in a 3D space may or may not intersect, so the algorithm firstly calculates the nearest points of those vectors. It then treats their centroid as an intersection when neither of the nearest points is equal to the reader's positions and the distance between the nearest points is less than certain threshold. Because an RFID reader with a single general antenna captures a wider area symmetrical around its direction, such intersections are distributed around the actual position of each RFID tag. The algorithm outputs a centroid of these intersections as an estimated position of each RFID tag. Algorithm 1 implements this concept.

In order to achieve high localization accuracy of RFID tags, reading records with various combinations of reader's position and direction are required. When they are biased toward a certain direction from an RFID tag, the localization error of the RFID tag increases in this direction in addition to a natural error as shown in Fig.3(b). However, in practice, it is difficult to obtain uniformly scattered reading records everywhere because of obstacles, such as walls or other factors. To remove such bias in the localization, a simple bias removal method with reference RFID tags can be applied on the localization algorithm. Placing some RFID tags at known positions as references, the localization algorithm can calculate amounts of errors in estimated positions of those RFID tags. The bias removal mechanism assumes an average of those signed errors

Algorithm 1 RFID localization algorithm : processing a reading record received from a smartphone

Input: new reading record i whose identifier is ID

$H \leftarrow$ list of the all reading records related to ID in database
for each reading record h in H **do**
  if reader's position/direction in i and h have an intersection (Fig.3(a)) **then**
    Store the intersection into the database
  end if
end for
if 1 or more new intersections are added **then**
  Update estimated position for ID with a centroid of its intersections in the database
end if
Store the input reading record i into the database

in each axis as the bias in localization, then subtracts it from estimated positions of other RFID tags.

Compared with the existing works described in Section II, our solution estimates positions of RFID tags with less information, therefore its localization error would be higher. However, it can still map the localization results to shelves or similar places whose positions are known when the distances between those locations is big enough against the error. This process is done by finding the nearest known place from the localization result of each RFID tag. The results will be presented in Section IV-B.

IV. Evaluation

We have evaluated the system in the following two steps. At first, the RFID localization algorithm described in Section III-B was implemented with Java and deployed on a cloud server with its backend database using MySQL. To prove the characteristics of the algorithm, we did an experiment where a RFID reader was placed at fixed positions. After that, we evaluated the performance of the whole system in a library. In both experiments we used a commercially-off-the-shelf low-cost RFID reader, JRM2030 from Shenzhen Jiuray Tech, China. The RFID reader conforms to EPC UHF Gen2 air protocol. In the second experiment, the mobile application ran on a Google Pixel2.

A. Accuracy evaluation on RFID localization algorithm with fixed-position reader

1) Experimental setup: In this experiment, 40 RFID tags were attached to a wooden shelf placed against a wall in authors' office room to emulate items on the shelf. As shown in Fig.4, the reader was placed in front of the shelf using a tripod, and connected to a computer controlling it.

Fig.5 illustrates the experimental setup, including the positions of the reader and tags. The following descriptions about this experiment use a 3-axis coordinate system with x, y and z axis corresponding to left-to-right direction looking from front of the shelf, direction away from the shelf, and height from

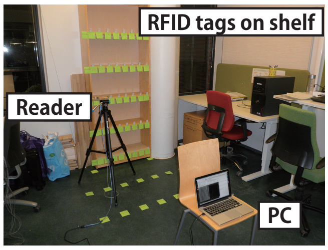

(a) Experimental setup

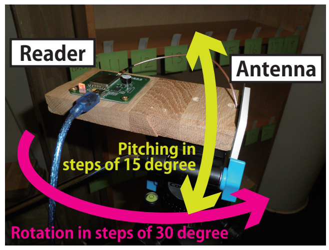

(b) RFID reader and antenna on the tripod

Fig. 4. Setup of the experiment with fixed-position readers

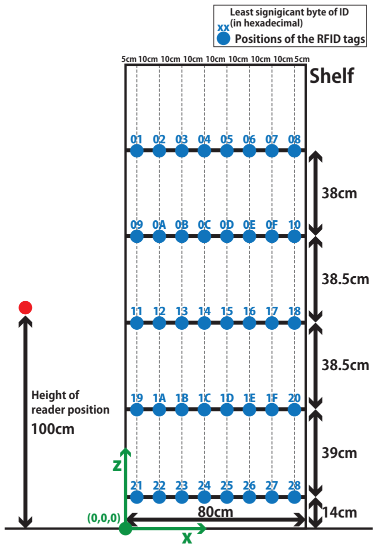

(a) Front view

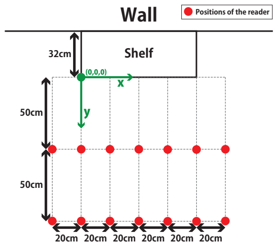

(b) Top view

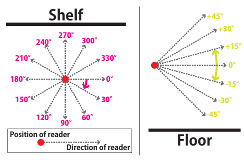

(c) Horizontal/vertical orientation of the reader at each fixed position

Fig. 5. Positions of the RFID reader and tags in the experiment with fixed-position reader.

the floor, respectively. The origin of the coordinate system is placed at a front-left corner of the shelf on the floor.

The shelf is 80cm wide and has 5 shelf boards with distance from the floor (z) of $14cm$, $53cm$, $91.5cm$, $130cm$ and $168cm$, respectively. 8 RFID tags were attached on edges of each shelf board with a 10cm interval, i.e. $x = 5, 15, 25, 35, 45, 55, 65, 75cm$ and $y = 0cm$. Each RFID tag has an unique serial number varying from "0x01" to "0x28" in hexadecimal as the least significant byte of its identifier. RFID tags between "0x01" and "0x08" were attached to the top shelf board ($z = 168cm$), and those between "0x09" and "0x10" were attached to the second shelf board ($z = 130cm$) in left-to-right order. Remaining RFID tags were also attached to the shelf in the same way.

The reader was placed at 14 positions which are combinations of $x = -20, 0, 20, 40, 60, 80, 100cm$, $y = 50, 100cm$ and $z = 100cm$. At each position, the horizontal orientation of the reader, i.e. $\arctan(y/x)$, was switched from $0°$ to $330°$ in steps of $30°$, where $0°$ means the right-hand side, looking from the front of the shelf. Vertical orientation of the reader, i.e. $\arctan(z/\sqrt{x^2 + y^2})$, was also changed from $45°$ to $-45°$

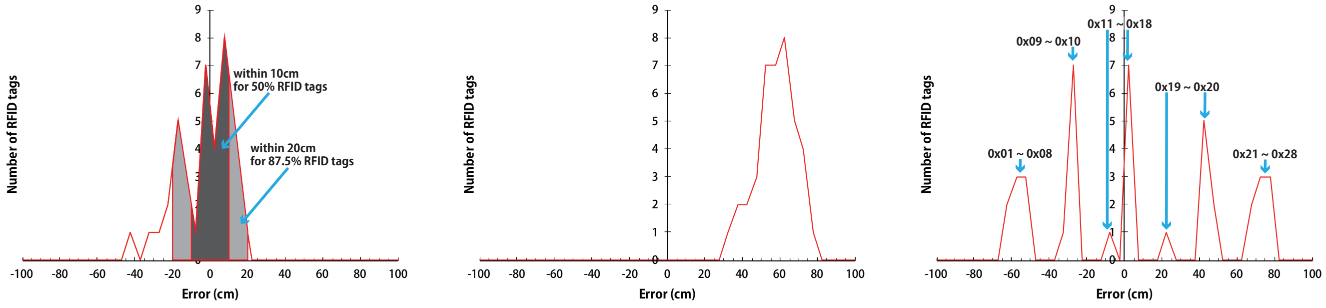

(a) x axis (b) y axis (c) z axis

Fig. 6. Distributions of RFID localization errors in the experiment using fixed-position RFID readers

in steps of 15° at each position and with each horizontal orientation, where 0° means being horizontal to the floor.

In this experiment, "inventory" (i.e. the process of obtaining identifiers of RFID tags in its reading range) was done for 1 second at each position and in each horizontal/vertical orientation of the reader. The obtained sets of read RFID tags' identifiers and reader's position and direction were fed to the localization algorithm. TPO of the reader was configured to $100mW$ ($= 20dBm$) considering future integration of readers into smartphones. For example, TRF7970A from Texas Instruments [25], which is an existing commercial NFC transceiver chip designed for mobile devices, has programmable $100mW$ and $200mW$ TPO, thus $100mW$ TPO can be considered as a feasible assumption for future UHF-band RFID readers in smartphones.

2) Expectations and results: This experimental setup has more variations of the reader's positions on the x axis in comparison with the y and z axes. Accordingly, it is expected that localization error on x axis would be smaller than those on other axes. On the other hand, the reader was placed at the same height, i.e. $z = 100cm$, throughout the experiment. It is expected that this uniform z value of the reader's position would result in higher localization error on the z axis, but variations in vertical direction of the reader still cause correlation between RFID tags' actual and estimated positions on the z axis. There are two variations of the reader's positions on the y axis, whereas both of them are located on the same side of the RFID tags. It is expected that this bias would also result in a higher localization error biased towards a certain direction on y axis as described in the section III-B.

In this experiment, 79027 reading records of the 40 RFID tags were collected in total. The localization errors of the RFID tags on each axis are summarized in Fig.6. An average of absolute error on the x axis is 11.5cm, which is smaller than those on the other axes. Figure 7(a) shows relationship between the actual and estimated positions of RFID tags on the x axis. Some of the RFID tags, such as "0x1F" and "0x28" have notably larger errors on the x axis than the other RFID tags. Those RFID tags were located near the floor, i.e. small z axis value, so it is considered that the localization accuracy has been affected by radio reflection from the floor. Because the

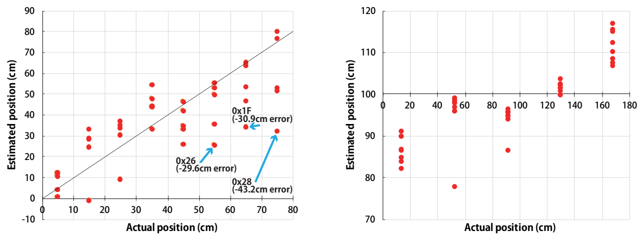

(a) x axis (b) z axis

Fig. 7. Actual positions vs. estimated positions of RFID tags with fixed-position RFID readers

proposal relies only on reading records which do not include any physical characteristics of radio waves, it cannot detect or eliminate any effects of multipath propagation and would therefore decrease localization accuracy.

Figure 6(b) and Figure 6(c) show larger errors on the y and z axis, which agrees to the above expectation. Errors in the y axis are strongly biased towards the reader's position, which also agrees to the expectation. Nevertheless, from Fig.7(b), the values for most of RFID tags located above the reader ($z = 100cm$) are estimated to be larger than $100cm$. Similarly, the z axis values for all the RFID tags located below the reader are estimated to be less than $100cm$. It means that the localization algorithm can estimate at least whether RFID tags are located above or below the reader, even if reader's height is fixed. Therefore, we consider that more measurement points on the z axis can achieve a higher localization accuracy in that axis. Errors in the y axis also can be reduced by applying the bias removal described in Section III-B

B. Evaluation on RFID mapping integrated with image-based localization

We evaluated the integrated RFID mapping system with experiments in our university's library. Figure 8 shows the experimental environment, with 2 double-sided shelves arranged at an angle. Each shelf has 4 segments and 5 rows on either side, and each cell is of 87cm width, 38cm height and 26cm depth. The bottom shelf boards are located at 12cm height. Note that the coordinate system arranged for an image-based

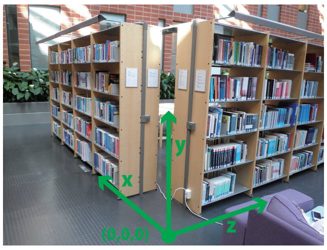

(a) Experimental environment and its coordinate system

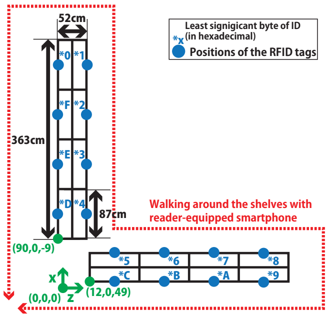

(b) Size and arrangement of shelves : top view

Fig. 8. Experimental environment for the integrated RFID mapping evaluation

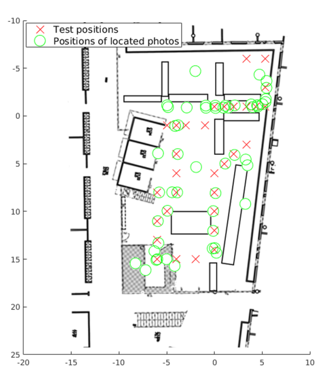

(a) Image-based localization

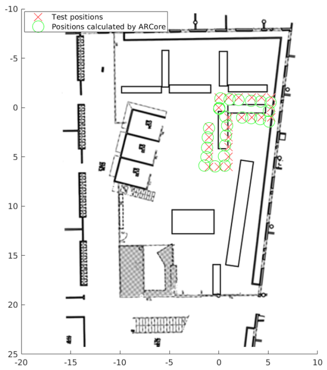

(b) ARCore tracking

Fig. 9. Positions where test photos were taken and their estimated positions overlaid on a library floor plan

Fig. 10. Examples of images that cannot be located by our system. Images were too close to obstacles or had insufficient distinctive visual features.

localization in the environment is different from that of the above fixed-reader experiment, i.e. the y axis corresponds to the height direction.

The remaining part of this section evaluates accuracy of image-based localization in the environment at first, then continues to evaluation of the integrated RFID mapping system.

1) Accuracy evaluation on image-based indoor localization: In this experiment we evaluate how well our initial localization and vision based tracking perform in the library. Before the experiment we have recorded a 6 minutes length video of the library and built an SfM model from the video. We have aligned the model to a metric coordinate system by taking a set of images at known locations and adding those images to the model.

We have selected 32 positions inside the library. We used a laser range finder to measure ground truth 3D coordinates at each position and took 4 photos at that position, each photo with 90° difference, starting from 0°. We then supplied all the images to image-based localization server to calculate their positions. Figure 9(a) shows test positions (red crosses) and calculated locations (green circles). Our localization system successfully located 80.9% of 128 images with mean position error of 1.09 m ($s = 1.43$) and mean facing direction error of 5.90° ($s = 9.24°$). Some images were not located because the photos captured too few visual details or were too close to obstacles (see Figure 10).

We have also evaluated ARCore based tracking inside the library. We have selected 25 positions around the shelves where we conducted RFID mapping and measured ground truth coordinates of the positions (see Figure 9(b)). We then aligned the phone with the initial position and started ARCore tracking. We moved the phone from one position to another and measured phone's estimated position and facing direction at each position. The tracking indicated a mean position error of 0.28 m ($s = 0.15$) and facing direction error of 2.84° ($s = 0.83°$). These correspond to the reader's position and direction errors in our experiment.

2) RFID mapping evaluation: For this experiment, a single RFID tag was assigned to each cell of the shelves, so in total 80 RFID tags with identifiers that contain serial numbers from "0x01" to "0x50" were used. RFID tags between "0x01" and "0x10" were attached to the top cells in their height direction, and those between "0x11" and "0x20" were attached to the second level cells. Remaining RFID tags were also attached to the shelf in the same way. The order of RFID tags attached to the cells in the same height is illustrated in Fig.8(b). Each RFID tag was attached to the center of the cell in its width/height direction and the outer surface in its depth direction. The procedure of the experiment is as the following.

1) First experimenter walked slowly around the shelves in both clockwise and counter-clockwise directions while carrying the reader-equipped smartphone as shown in Fig.8(b). While walking, the experimenter moved the smartphone to aim its camera at each of the all RFID tags. The smartphone performs continuous "inventory" operation and image-based localization of itself, then sends identifiers of read RFID tags and its position/direction to the RFID localization algorithm.
2) Second experimenter walked around the shelves in the same way. Two experimenters are of different heights thus making a variation in height position of the reader.
3) We defined the above two processes as a "round", then repeated it 3 times. Results of RFID localization at the end of each round were recorded to examine changes in accuracy with increasing number of reading records.
4) We repeated the above processes by setting the reader's TPO to $100mW$ and $200mW$, respectively. These conditions were chosen based on the existing NFC transceiver product as described in the previous fixed-position reader experiment.

Accuracy variation against TPO and number of experimental rounds: Table II summarizes average error of

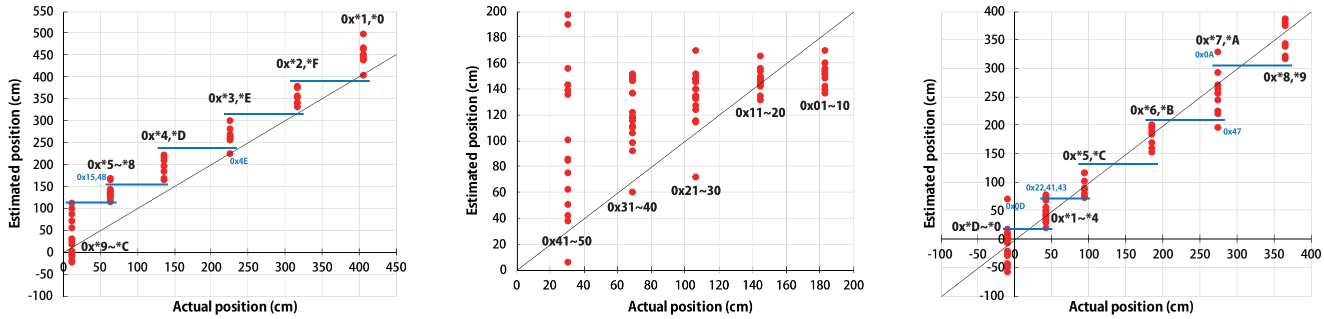

(a) x axis (b) y axis (c) z axis

Fig. 11. Actual positions of RFID tags vs. the positions estimated by our solution: Red points denote relationships between actual and estimated positions of RFID tags. Black numbers on each group of red points denote corresponding identifiers of RFID tags, i.e. location described in Fig.8(b). In the x and z axes, the groups of red points can be clearly separated by their estimated positions, which is denoted by a blue line, except some RFID tags are denoted by blue numbers. It means the order of RFID tags can be correctly detected in most cases based on the estimated positions on these axes.

TABLE II
AVERAGE ERROR OF RFID LOCALIZATION IN DIFFERENT CONDITIONS

TPO (mW)	No. reading records in each round		Average of absolute error (cm) x	y	z	Euclidean
100	1	19764 records	47.3	39.0	20.4	71.3
	2	39647 records	72.5	42.5	21.5	94.1
	3	58472 records	67.3	41.2	17.1	87.1
200	1	21397 records	57.1	38.2	16.7	77.2
	2	42416 records	59.2	36.9	14.8	77.5
	3	63779 records	59.0	40.4	16.0	80.1

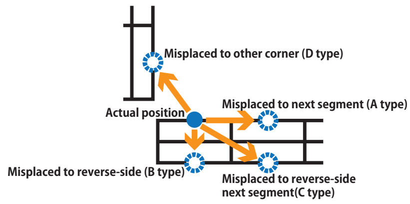

Fig. 12. Types of errors in the process of locating RFID tags in different segments of the shelves

TABLE III
LOCALIZATION ERROR WITH/OUT BIAS REMOVAL

Type of estimation result	Number of RFID tags without bias removal	with bias removal
correct estimation	52(65.0%)	63(84.0%)
A type error	16(20.0%)	7(9.3%)
B type error	6(7.5%)	4(5.3%)
C type error	1(1.3%)	0(0.0%)
D type error	5(6.3%)	1(1.3%)
total	80	75

RFID localization in each experiment setup. Average error on each axis and that in Euclidean distance are shown in the table. In this result, the accuracy of localization does not have correlation with the number of experimental rounds (reading records), thus it is considered that the reading records collected in only the first round are already enough for the localization. From the TPO perspective, $200mW$ TPO results in more stable localization than $100mW$ condition, but the amount of error in those conditions have a small difference. Therefore, in the following detailed analysis, a localization result obtained from the first experimental round of $100mW$ TPO condition is selected as a representative due to its lowest cost in both time and power consumption in measurements.

Errors in the orders of RFID tags: Figure 11 shows estimated positions of RFID tags under the above-mentioned condition. While the estimated positions on the x axis are biased towards its positive direction, the orders of the RFID tags are correctly detected as shown in Fig.11(a) and 11(c), respectively. When the width of a shelf segment is $90cm$, 77 RFID tags out of 80 can be mapped to the correct shelf segments, which the 4 groups on the right side in Fig.11(a) and 11(c) correspond to. From the perspective of sides of double-sided shelves, i.e. $52cm$ wide shelf segments, which 2 groups on the left side in Fig.11(a) and 11(c) correspond to, 79 RFID tags out of 80 can be ordered correctly. In total, 9 RFID tags marked in the figures have an error affecting the order, but the other 71 RFID tags are localized within a tolerable error for a correct ordering in this experiment setup. On the other hand, on the y axis, corresponding to the height from the floor, the amount of error and its distribution width are too large to order RFID tags correctly on the axis. In contrary to large variation of smartphone's position on the floor plane, even if the experimenters moved up and down the smartphone while walking, the variation of its height is still smaller than that of arranged RFID tags. This causes larger error in the height direction thus making it difficult to detect the correct order.

Locating RFID tags in shelf segments: The above ordering evaluation shows that the range of localization error on the floor plane, i.e. x and z axes, is small enough for most of RFID tags to identify shelf's segments where they are placed. However, there is still a problem of biased localization, especially on the x axis. The bias removal with reference RFID tags is applied to evaluate its performance. In this evaluation, 5 RFID tags in the same segment (0x01, 0x11, 0x21, 0x31, 0x41) are chosen as reference RFID tags. After applying the bias removal, the average errors of localization in the x, y,

z axes and Euclidean distance change to $27.4cm$, $36.5cm$, $22.5cm$ and $58.4cm$, respectively. There are a few changes in the y and z axes, but the error in x axis is reduced and it affects the error in Euclidean distance. Table III summarizes results of the estimation which assumes RFID tags are placed at the segment closest to their estimated positions. Figure 12 illustrates types of errors observed in this experiment. The table shows that the bias removal improves the accuracy of the estimation. It greatly reduces the estimation errors in case of $90cm$ wide shelf segment (A type "next segment" error), and also cancels some of the errors in case of $52cm$ wide shelf segment (B type "reverse-side segment" error). As a result, 84% of RFID tags out of 75 (5 reference RFID tags are excluded) are located to the correct segments of the shelves.

V. Conclusion

This paper proposed a low cost solution that maps and locates RFID tags in a 3D space with reader-equipped smartphones. It combines relative RFID tag localization with image-based localization of smartphones, and supports bias removal using reference RFID tags. The proposal achieves on average $25cm$ accuracy in the localization of RFID tags along each of the orthogonal axes on the floor plane, and detects over 80% of RFID tags in the correct order. This accuracy may not be higher than those of the state-of-art solutions, but it is important to note that the proposal relies only on smartphones' cameras and "inventory" function of RFID readers, which can be considered as the minimum functionality of future reader-equipped smartphones.

Acknowledgement

This work was partially supported by a mobility scholarship of the author at Aalto University in the frame of the Erasmus Mundus Action 2 Project TEAM Technologies for Information and Communication Technologies, funded by the European Commission. It was also partially supported by the Advanced Connectivity Platform for Vertical Segments project, funded by European Institute of Innovation and Technology. This publication reflects the view only of the author, and the Commission cannot be held responsible for any use which may be made of the information contained therein.

References

[1] L. Shangguan, Z. Yang, A. X. Liu, Z. Zhou, and Y. Liu, "Stpp: Spatial-temporal phase profiling-based method for relative rfid tag localization," *IEEE/ACM Trans. Netw.*, vol. 25, no. 1, pp. 596–609, Feb. 2017. [Online]. Available: https://doi.org/10.1109/TNET.2016.2590996

[2] Impinj, "xArray RAIN RFID Gateway." [Online]. Available: https://www.impinj.com/platform/connectivity/xarray/

[3] Y. Ma, N. Selby, and F. Adib, "Minding the billions: Ultra-wideband localization for deployed rfid tags," in *Proceedings of the 23rd Annual International Conference on Mobile Computing and Networking*, ser. MobiCom '17. New York, NY, USA: ACM, 2017, pp. 248–260. [Online]. Available: http://doi.acm.org/10.1145/3117811.3117833

[4] J. Ryoo and S. R. Das, "Phase-based ranging of rfid tags with applications to shopping cart localization," in *Proceedings of the 18th ACM International Conference on Modeling, Analysis and Simulation of Wireless and Mobile Systems*, ser. MSWiM '15. New York, NY, USA: ACM, 2015, pp. 245–249. [Online]. Available: http://doi.acm.org/10.1145/2811587.2811620

[5] M. Noreikis, Y. Xiao, and A. Ylä-Jääski, "Seenav: Seamless and energy-efficient indoor navigation using augmented reality," in *Proceedings of the on Thematic Workshops of ACM Multimedia 2017*. ACM, 2017, pp. 186–193.

[6] Z. Rashid, R. Pous, J. Melià-Seguí, and M. Morenza-Cinos, "Mobile augmented reality for browsing physical spaces," in *Proceedings of the 2014 ACM International Joint Conference on Pervasive and Ubiquitous Computing: Adjunct Publication*, ser. UbiComp '14 Adjunct. New York, NY, USA: ACM, 2014, pp. 155–158. [Online]. Available: http://doi.acm.org/10.1145/2638728.2638796

[7] W. Zhang, Y. Lu, Y. Meng, and H. Yu, "Easy picker: Picking objects aided by passive rfids," in *Proceedings of the 13th International Conference on Ubiquitous Computing*, ser. UbiComp '11. New York, NY, USA: ACM, 2011, pp. 573–574. [Online]. Available: http://doi.acm.org/10.1145/2030112.2030219

[8] M. Miyazawa, Y. Igarashi, and J. Mitsugi, "A feasibility study of plug-in type rf tag localization system for handheld uhf rfid reader/writers," in *2015 21st Asia-Pacific Conference on Communications (APCC)*, Oct 2015, pp. 680–685.

[9] L. Shangguan and K. Jamieson, "The design and implementation of a mobile rfid tag sorting robot," in *Proceedings of the 14th Annual International Conference on Mobile Systems, Applications, and Services*, ser. MobiSys '16. New York, NY, USA: ACM, 2016, pp. 31–42. [Online]. Available: http://doi.acm.org/10.1145/2906388.2906417

[10] Y. Zhang, L. Xie, Y. Bu, Y. Wang, J. Wu, and S. Lu, "3-dimensional localization via rfid tag array," in *2017 IEEE 14th International Conference on Mobile Ad Hoc and Sensor Systems (MASS)*, Oct 2017, pp. 353–361.

[11] G. Shi and Y. Ming, "Survey of indoor positioning systems based on ultra-wideband (uwb) technology," in *Wireless Communications, Networking and Applications*. Springer, 2016, pp. 1269–1278.

[12] C. Yang and H.-R. Shao, "Wifi-based indoor positioning," *IEEE Communications Magazine*, vol. 53, no. 3, pp. 150–157, 2015.

[13] Y. Zhuang, J. Yang, Y. Li, L. Qi, and N. El-Sheimy, "Smartphone-based indoor localization with bluetooth low energy beacons," *Sensors*, vol. 16, no. 5, p. 596, 2016.

[14] Z. Liu, L. Zhang, Q. Liu, Y. Yin, L. Cheng, and R. Zimmermann, "Fusion of magnetic and visual sensors for indoor localization: Infrastructure-free and more effective," *IEEE Transactions on Multimedia*, vol. 19, no. 4, pp. 874–888, 2017.

[15] J.-Y. Huang, S.-H. Lee, and C.-H. Tsai, "A fast image matching technique for the panoramic-based localization," in *Computer and Information Science (ICIS), 2016 IEEE/ACIS 15th International Conference on*. IEEE, 2016, pp. 1–6.

[16] G. Gerstweiler, E. Vonach, and H. Kaufmann, "Hymotrack: A mobile ar navigation system for complex indoor environments," *Sensors*, vol. 16, no. 1, p. 17, 2015.

[17] J. Ventura, C. Arth, G. Reitmayr, and D. Schmalstieg, "Global localization from monocular slam on a mobile phone," *IEEE transactions on visualization and computer graphics*, vol. 20, no. 4, pp. 531–539, 2014.

[18] J. Dong, Y. Xiao, M. Noreikis, Z. Ou, and A. Ylä-Jääski, "imoon: Using smartphones for image-based indoor navigation," in *Proceedings of the 13th ACM Conference on Embedded Networked Sensor Systems*. ACM, 2015, pp. 85–97.

[19] N. Snavely, "Bundler: Structure from motion (sfm) for unordered image collections," 2006.

[20] C. Wu *et al.*, "Visualsfm: A visual structure from motion system," 2011.

[21] P. Moulon, P. Monasse, R. Perrot, and R. Marlet, "Openmvg: Open multiple view geometry," in *International Workshop on Reproducible Research in Pattern Recognition*. Springer, 2016, pp. 60–74.

[22] D. G. Lowe, "Distinctive image features from scale-invariant keypoints," *International journal of computer vision*, vol. 60, no. 2, pp. 91–110, 2004.

[23] Mojix, "STAR RFID Reader." [Online]. Available: https://www.mojix.com/star-content/

[24] F. Schaffalitzky, A. Zisserman, R. I. Hartley, and P. H. Torr, "A six point solution for structure and motion," in *European Conference on Computer Vision*. Springer, 2000, pp. 632–648.

[25] Texas Instruments, "TRF7970A Multi-Protocol Fully Integrated 13.56-MHz NFC / RFID Transceiver IC." [Online]. Available: http://www.ti.com/product/TRF7970A